Poster2-12

X-band Phased Array Weather Radar Observations of a Mesocyclone in the Tokyo Urban Area

S. Shimamura*, K. Morotomi, S. Kurihara (Japan Radio Co., Ltd., Nagano, Japan)
F. Kobayashi (National Defense Academy, Kanagawa, Japan)
T. Takano, A. Higuchi, T. Takamura (Chiba University, Chiba, Japan)
H. Iwashita (Meisei Electric Co., Ltd., Gunma, Japan)

1. INTRODUCTION

In summer, around Tokyo urban area in Japan, localized heavy rainfall, downburst, and lightning sometimes threaten lives [1] [2]. These severe weather events can be brought down from cumulonimbi above. Cumulonimbi, growing three-dimensionally and rapidly in several or several ten minutes, cause such events onto the ground. For prediction and detection of the events, weather radar is required to achieve rapid and three-dimensional scanning. Conventional radars with parabolic antennas, however, are capable of scanning with temporal resolution of 5 minutes of limited lower angles. Japan Radio Co., Ltd. has developed a phased array weather radar (PAWR) [3]. With this phased array weather radar, it takes only 30 seconds to finish a volume scan of the cylindrical space with a radius of 80 km and height of 20 km.

This paper introduces a mesocyclone which brought down heavy rain and downburst on August 27th 2018 by using PAWR observation data. Three-dimensional structure of the mesocyclone and utility of PAWR on detection and prediction of the downbursts are discussed.

2. JRC'S PHASED ARRAY WEATHER RADAR

To solve insufficiency of conventional radar observation, a PAWR system [4] with rapid, full-volume scanning was required. After 2012, six PAWR systems were installed in Japan, which include five single-polarization PAWR and one dual-polarization's.

Japan Radio Co., Ltd. independently developed a prototype of weather radar equipped with an active phased array antenna in 2015 [3]. Our phased array antenna system adopts digital beamforming technique. With this technique, the radar simultaneously forms multiple pencil receive beams in a fan-shaped transmit beam. By electrically changing elevation angle, single vertical scan of almost whole elevation angles finishes in just a moment. The PAWR, installed in Chiba city (Figure 1), started to observe in summer in 2015. The observation area of the radar includes the Tokyo urban area.

3. MESOCYCLONE OBSERVATION ON AUGUST 27, 2018

3.1 Overview

Tokyo Regional Headquarters reported that on August 27, 2018, due to a stationary front located around the North part of Japan and temperature rising in the day time, warm moist air blew up from the Pacific Ocean to the Tokyo urban area. In this evening, atmospheric conditions were getting unstable. After 19:00 on JST, there were heavy rain, hailstorm, and lightning in Nerima and Setagaya in the urban area. An

Fig. 1 Appearance and Observation Area of JRC's PAWR

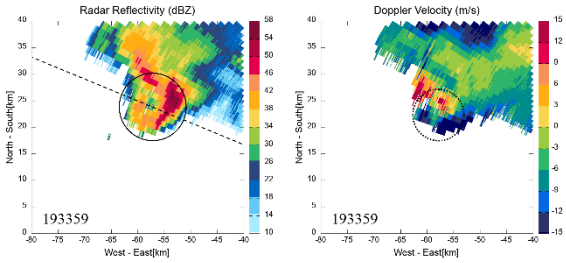

Fig. 2 The PAWR reflectivity and Doppler velocity field on 19:33:59 JST at 5km altitude (a) Reflectivity (Solid black circle indicates the ring shape echo. Dashed black line indicates an axis of the cross section in Fig. 3), and (b) Doppler velocity field (Dotted black circle indicates the couple of positive and negative Doppler velocity

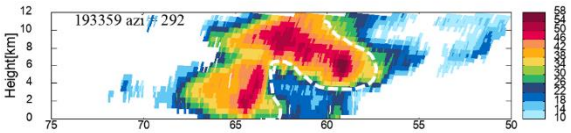

Fig. 3 The vertical section of the PAWR reflectivity on 19:33:59 at an azimuth angle of 292° along the dashed black line in Fig. 2 (a) (Dashed white line indicates the boundary of strong echo and weak echo areas).

* *Corresponding author address:* Shigeharu Shimamura, Japan Radio Co., Ltd., Dept. of Research and Development, Nagano-shi, Nagano 381-2289; e-mail: shimamura.shigeharu@jrc.co.jp

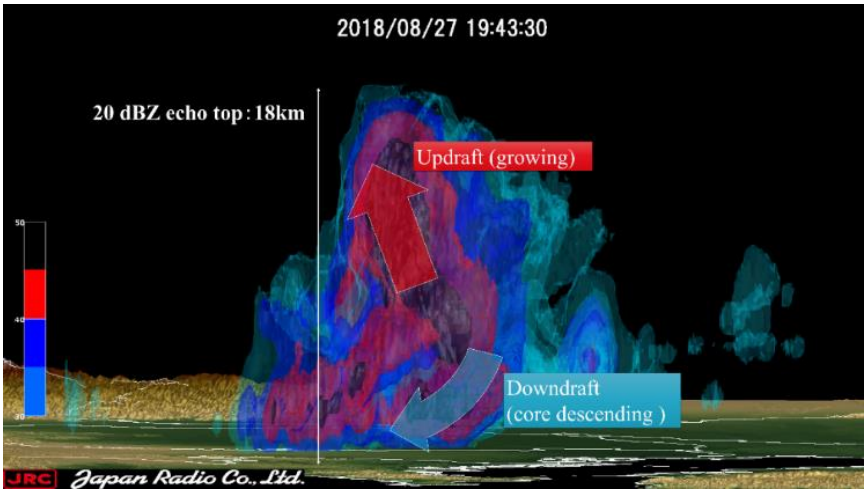

Fig. 4 3D structure of the cumulonimbus observed by the PAWR on 19:43:30 JST

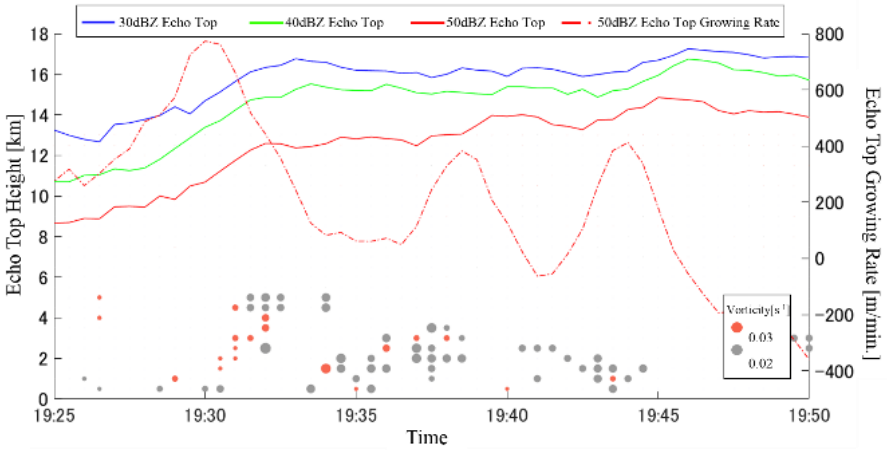

Fig. 5 The time-height section of vorticity and the time series of the PAWR echo top height on 30, 40, and 50 dBZ, and echo top growing rate on 50 dBZ.

Automated Meteorological Data Acquisition System (AMeDAS) at Nerima recorded a rainfall rate of 74mm/h between 19:30 to 20:30 JST and a strong North wind velocity of 25.1m/s on 19:46 JST. At that time, floods, fallen trees and electric shortage were reported in Nerima and Setagaya. According to the field survey, the gust of wind was probably caused by a downburst which had been originated from a mesocyclone above.

This chapter introduces three types of analysis results by using our PAWR observation data.

3.2 3D structure of cumulonimbus

Figure 2 displays horizontal distributions of radar reflectivity and the Doppler velocity field at 5 km height by the PAWR on 19:34:00 JST. In this figure, attributes of a mesocyclone, in particular, a ring shape of radar reflectivity in the solid black circle and a couple of positive and negative Doppler velocities in the dotted black circle are shown. In the Doppler velocity field, positive regions indicate precipitation particles moving away from the PAWR, whereas negative regions indicate them moving towards to the radar, which implies the couple of velocities here suggests the vortex's rotation was counterclockwise. Figure 3 shows a vertical cross section of the convective system which moved roughly from left to right. A vault-like shape of radar echoes that strong radar echo areas (red or yellow colored) are surrounding the upper side of weak echo area (green colored area) are shown. The boundary of the areas is indicated by the dashed white line. This echo shape implies that strong updrafts blowing up from the front-side of the system existed at the weak echo region in the vault. Figure 4 shows a 3D image of the twisted cloud echo looking from the South side on 19:43:30 JST, revealing that the convective cloud had approximately 18 km of 20 dBZ echo top height at maximum and three-dimensionally tornadic form. At that time, in the cloud, both updraft and downdraft co-existed, which were separated and had skew positions each other. Because of the twisted form, they did not cancel out each other, and convective growth and precipitation core's descending co-existed in the same system.

According to these observation images, the convective cloud, bringing downburst onto the ground, had structural characteristics of, generally known as, a super cell and a mesocyclone.

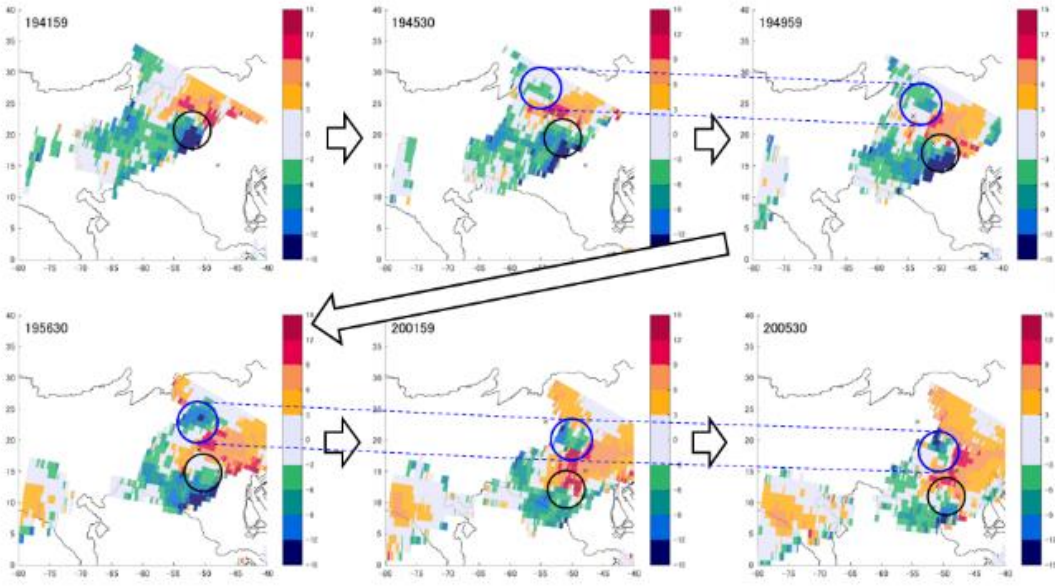

Fig. 6 The PAWR Doppler velocity field from 19:41:59 to 20:05:30 at 0.5 km altitude (A solid black circle indicates the locations of the Doppler velocity pairs, and a solid blue circle indication the locations of green colored wind component)

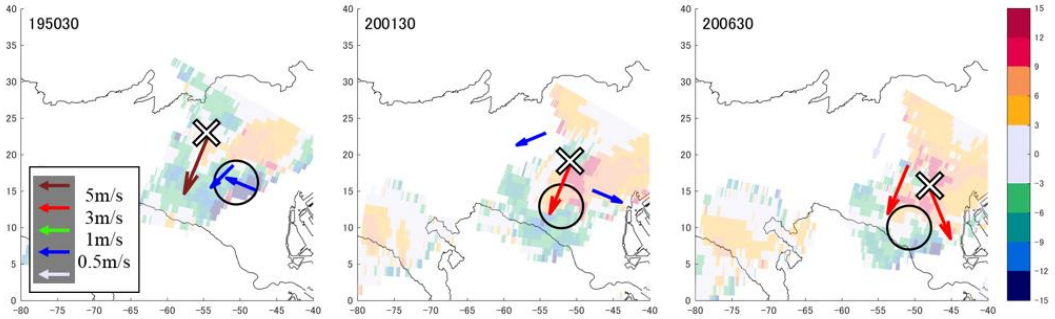

Fig. 7 Wind directions and velocities on the surface by three POTEKAs at time green colored wind component reached at the POTEKA site pointed by the cross mark over the Doppler velocity fields at 0.5km altitude with light colors

3.3 Vorticity in storm cell

To investigate time-height structure of the storm, we derived time-height sections of pseudo vertical vorticities of the vortex calculated individually from the PAWR Doppler velocity field data. Figure 5 shows time series of echo top height on each radar reflectivity and the echo top growing rate line only at 50 dBZ as well as time-height sections of vorticity. Since the 30 dBZ echo top height (solid blue) and the 50 dBZ echo top height (solid red) reached at approximately 17 km and over 14 km, respectively, this storm can be estimated as one of the most intense localized weather phenomena in these years in Japan, as hazardous as "Nerima Heavy Rain" in 1999 [1]. Furthermore, the 50 dBZ echo top growing rate (dashed red) reached to approximately 800 m/min. on 19:30:00 JST. This growing rate also implies growing process of the cloud cell was extremely rapid and the process cannot be detected by conventional weather radars whose temporal resolutions are 5 to 10 minutes. On the other hand, the cell had strong vertically-successive vorticities over 0.02 s^{-1} which probably played a role to roll up precipitation particles and water vapor around it and to promote its growth. This state of strong vorticities continued from 19:30 to 19:45 JST approximately. Since the estimated vorticity values in the storm exceeded 0.01 s-1 which is general criteria of the mesocyclone, the storm can be defined as a mesocyclone. Focusing on a relation between echo top growing rate and vorticity, at the three times on the local maximums of the growing rate, 19:30:00, 19:38:00, and 19:44:00 JST, strong vorticities were continuously detected. Consequently, this relation suggests that vertical vorticity can be related to growth of convective clouds.

3.4 Downburst

As referred in the Chap. 3. 1, a strong gust wind of 25.1 m/s, contributed by a downburst, was recorded on 19:46 JST in Nerima. Figure 6 shows every 3 or 4 minutes' Doppler velocity fields at 0.5km altitude around the time of the downburst occurrence (19:46 JST). A region with wind components toward the PAWR colored by green appeared in a blue circle on

19:45:30 JST. The location of the Doppler components was at the North side of the positive and negative Doppler velocity pair in a black circle. The green color region, gradually growing larger, chased after the Doppler velocity pair caused by the mesocyclone, moving from North to South. Since firstly appeared on 19:45:30 JST which was just the time of the downburst occurrence, the region likely indicates a part of the downburst outflow. In order to establish the hypothesis, two-dimensional wind velocity data on ground surface is compared to the PAWR Doppler velocity field data. POint TEnki KAnsoku in Japanese (POTEKA) [5] developed by Meisei Electric Co., Ltd. can observe every minute's seven meteorological variables including mean wind velocity and its direction. In Figure 7, arrows show wind velocities and directions recorded by three POTEKAs equipped along the track of the mesocyclone. According to the dataset, arrival of the green Doppler velocity region and measurements of mean wind velocities over 3 m/s with the North direction on each POTEKA sites coincided within a minute. This coincidence likely imply that the wind components at the backside of the mesocyclone seen in the PAWR's Doppler velocity fields were parts of the downburst outflow.

4. DISCUSSION

4.1 Mechanism of the downburst outbreak

The mesocyclone brought about heavy rain, hail, and finally strong winds over 25 m/s. A twisted structure of the vortex that updraft and downdraft were located in separately, developing precipitation particles larger for a long time, resulted in hailstorm. By falling down from higher level, large raindrops and hailstones, pulling down ambient air [6], caused strong downdrafts, and finally resulted in the downburst on 19:46 JST.

Although explanation and image are abbreviated, a notch of the radar reflectivity at 5 km height was shown at the Northwest of the mesocyclone, which is presumed to be mid-level dry air inflow [6]. Also this inflow that firstly appeared 19:20 JST and the downdrafts by precipitation particles could gradually strengthen the downdraft.

4.2 Unclarified issues

In a supercell storm including a mesocyclone, a precipitation area including hailstorm experimentally is at forward side of a vortex. At the extreme precipitation area, a downward air current occurs called forward flunk downdraft (FFD) [7]. Nevertheless, in this event, strong precipitation area was at backward side rather than forward side. Since the location of the downburst was also at the North of the mesocyclone which was backside facing the direction of the mesocyclone migration, the downburst can be influenced by rear flunk downdraft (RFD) [8]. After the downburst, echo shapes of rear flunk down draft internal surge (RFDIS) was also observed. Both RFD and RFDIS are strongly related to tornado development. However, in this event, tornado did not occur. In order to clarify a mechanism of forming mesocyclone and the reason of no tornado, more detailed analysis such as multi Doppler analysis by multiple PAWRs and change of wind field on ground is required.

5. CONCLUSION

This paper reports three-dimensional analysis on the mesocyclone around the Tokyo urban area on August 27, 2018. Spatial structures of the vortex and its rapid growing process were revealed by the PAWR's three-dimensional rapid scanning. The vorticity analysis provided a potential to predict rapid growth of cumulonimbi and occurrence of downburst by monitoring low-level vorticities.

A networked radar environment is more suitable for mesocyclone detection system because attenuation correction [9], multiple Doppler analysis instead of pseudo vorticity estimation derived by individual Doppler analysis can be achieved.

Reference

[1] Seko, H., et al., 2007: Evolution and air flow structure of a Kanto thunderstorm on 21 July 1999 (the Nerima Heavy Rainfall Event). *Journal of the Meteorological Society of Japan*. Ser. II, 85, 4, 455-477.

[2] Sakurai, N., et al., 2018: Development of lightning indices using TOKLMA and X-band polarimetric radar network during the summer season in Tokyo metropolitan area, *16th International Conference on Atmospheric Electricity*, Oral, 09, 02.

[3] Kashiwayanagi, T., et al., 2016: Rapid 3D scanning high resolution X-band weather radar with active phased array antenna, *Tech. Conf. on Meteorological and Environmental Instruments and Methods of Observation*.

[4] Mizutani, F., et al., 2018: Fast-scanning phased-array weather radar with angular imaging technique, *IEEE Transactions on Geoscience and Remote Sensing*, 56, 5, 2664-2673.

[5] Iwashita, H., et al., 2019: Downburst observations by a high density ground surface observation network (POTEKA), *Journal of Atmospheric Electricity*, 38, 1, 23-35.

[6] Adachi, T., et al., 2016: High-speed volumetric observation of a wet microburst using X-band phased array weather radar in Japan, *AMS Monthly Weather Review*, 144, 10, 3749-3765.

[7] Lemon, Leslie R., et al., 1979: Severe thunderstorm evolution and mesocyclone structure as related to tornadogenesis, AMS *Monthly Weather Review*, 107, 9, 1184-1197.

[8] Lee, Bruce D., et al., 2012: The Bowdle, South Dakota, cyclic tornadic supercell of 22 May 2010: Surface analysis of rear-flank downdraft evolution and multiple internal surges, *AMS Monthly Weather Review*, 140, 11, 3419-3441.

[9] Shimamura, S., et al., 2016: Probabilistic attenuation correction in a networked radar environment, *IEEE Transactions on Geoscience and Remote Sensing*, *54*, 12, 6930-6939.